JOURNAL OF MATERIALS SCIENCE **34** (1999) 3685–3693

Grinding effects of host crystals on formation and properties of titania pillared fluorine micas

T. YAMAGUCHI*, F. KUNIYOSHI, K. KITAJIMA
Department of Chemistry and Material Engineering, Faculty of Engineering, Shinshu University, Wakasato, Nagano 380-8553, Japan
E-mail: mtmouth@gipwc.shinshu-u.ac.jp

Fluorine micas having different grinding times were allowed to react with titania sol prepared by hydrolyzing titanium tetraisopropoxide (TTIP) with hydrochloric acid in order to clarify the influence of grinding upon reactivity of synthetic fluorine micas [$M_{0.8}Mg_{2.2}Li_{0.8}(Si_4O_{10})F_2$ (M = Na, Li)]. Prolongation of grinding time promoted delamination and fineness of host mica crystals, resulting in increasing specific surface area. The heating weight loss and intensity of IR absorption bands around 1600 and 3400 cm^{-1} also increased with increasing grinding time, indicating the increase in absorbed water on ground mica particles. Properties of titania pillared fluorine micas depended on grinding time of host micas. Specific surface areas and titania contents of pillared fluorine micas increased with increasing grinding time, so that the effect of interlayer cations (Na^+, Li^+) upon complex formation of titania pillared micas almost diminished. When host mica crystals were larger, the reaction occurred mainly in the interlayer region. However, when host mica crystals were ground to be finer, the reaction on external surfaces of ground particles occurred simultaneously along with intercalation. These results show that mechanochemical effects resulted from grinding have the profound influence on the formation and properties of titania pillared fluorine micas.

1. Introduction

Pillared clays are two-dimensional microporous materials. They are prepared by propping open the clay layers through the introduction of metal oxide pillars in the interlayer region. Titania pillared fluorine micas are attractive solids for adsorption and catalysis purposes due to their high surface area and porosity. They have sinterability at high temperature to yield useful sintered bodies (ceramics) and nanocomposites. They are promising environmental materials because titania has photochemical reactivity.

The present authors have reported on synthesis of titania pillared fluorine micas from expandable fluorine micas having different layer charges and interlayer cations, such as Li^+, Na^+ and K^+, with titania sol [1]. The formation and properties of titania pillared fluorine micas thus obtained are affected by expandability of host mica crystals. In general, expandable fluorine micas have higher crystallinity and larger cation exchange capacity (CEC) than smectites, such as montmorillonite. We have found that the reactivity of titania sol with taeniolite series fluorine micas having interlayer Na^+ is much lower than that having interlayer Li^+. The reason is (i) that the taeniolite series fluorine mica having the interlayer cation of Na^+ exhibits limited swelling and (ii) that the size of mica crystals is too large for titania sols to diffuse into the central cores of each crystals because intercalation is determined by the two-dimensional controlled process.

Mechanochemical effects [2–4] on layered silicates such as muscovite and montmorillonite have been intensively studied but mechanochemical effects on synthetic fluorine micas have not been reported up to now. Surface activation as well as decreasing particle size and increasing specific surface area has been expected to occur upon grinding mica crystals. Therefore, we have attempted to react fluorine micas having different grinding times with titania sol to clarify the effects of grinding host mica crystals. Consequently, the reactivity of mica crystals with titania sol and properties of titania pillared micas thus obtained have been found to change with the grinding time of host mica crystals. In the present paper, the particle sizes of host micas are represented by their specific surface areas calculated from isotherms for nitrogen at liquid nitrogen temperature since it is difficult to estimate the host particle sizes because of their swellability with water.

2. Experimental

The starting Na and K taeniolite series micas having layer charge of 0.8, $Na_{0.8}Mg_{2.2}Li_{0.8}Si_4O_{10}F_2$ and $K_{0.8}Mg_{2.2}Li_{0.8}Si_4O_{10}F_2$, were synthesized by the same melting procedure as described previously [5]. Crystal

* Author to whom all correspondence should be addressed.

aggregates thus obtained were crushed and classified to obtain the particles of 44–74 μm (hereafter denoted by $W_{0.8}$-tae, where W = Na or K). The crushed micas were then ground manually by an agate mortar for 1, 3, 5 and 7 h (hereafter abbreviated to 1h-, 3h-, 5h- and 7h-$W_{0.8}$-tae respectively, where W = Na or K). A portion of the ground Na micas were transformed into the homoionic Li^+-exchanged forms (hereafter abbreviated to 1h, 3h, 5h and 7h-$Li_{0.8}$-tae, respectively) by repeated treatments with 2 mol/l LiCl aqueous solution. Each mica was characterized by the measurements of thermogravimetric (TG) curve, infrared (IR) spectra and BET surface area.

The titania sol was prepared by hydrolyzing titanium tetraisopropoxide (TTIP) with hydrochloric acid [6]. The molar ratio [HCl/TTIP] was 4 using 1 mol/dm^3 HCl. The clear sol thus obtained was stirred for 3 h at room temperature.

Separate samples of the ground micas dispersed in distilled water (1 wt %) were mixed and allowed to react with the titania sol at 50 °C for 180 min. After the reaction, the products were centrifuged, and followed by repeated washing with water to remove excess sol. The samples (hereafter abbreviated to 1h-$Na_{0.8}$-Ti-tae for example) were dried in air. X-ray diffraction (XRD) patterns were recorded on the air-dried samples and the products heated at 150–800 °C for 2 h in air by using CuK_α radiation. Surface areas and pore size distributions of the same samples were evaluated from adsorption-desorption isotherms for nitrogen at liquid nitrogen temperature. Prior to the isotherm measurement, all the samples were degassed by evacuation at 150 °C. The contents of TiO_2 were determined by the titration method [7] with $FeCl_3$ standard solution after the samples were fused with the mixture of NaOH and Na_2O_2.

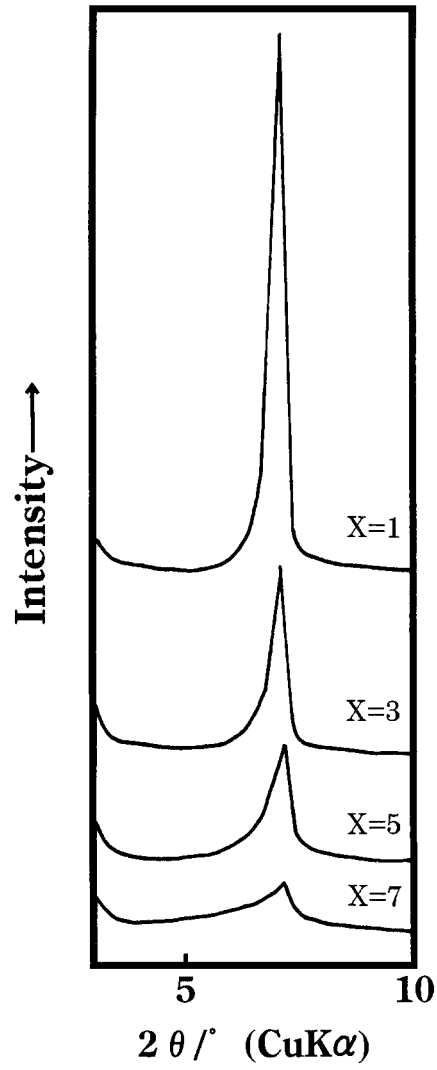

Figure 1 XRD patterns of $Na_{0.8}$-taeniolite having different grinding times. The value of *x* shows the grinding time.

3. Results and discussion

3.1. Changes in the properties of mica crystals with grinding

Fig. 1 shows the change in XRD patterns of 001 reflection regions for $Na_{0.8}$-taeniolite having different grinding times. The (001) peak at 7.2° (CuK_α) decreased in intensity and broadened with increasing grinding time. These results indicate that the prolongation of grinding time promotes delamination and fineness of host mica crystals. In addition, BET specific surface area increased considerably with increasing grinding time. 1h- and 7h-$Na_{0.8}$-tae exhibited the surface area of 22.4 and 129.0 $m^2\ g^{-1}$, respectively.

Fig. 2 shows TG curves of $K_{0.8}$-, $Na_{0.8}$- and $Li_{0.8}$-tae having different grinding times. Thermal weight loss characteristics changed with changing interlayer cations in mica crystals. The weight loss decreased in the order of the interlayer cation species $Li^+ > Na^+ > K^+$, due to the amount of interlayer water molecules related to the difference in expandability. The weight loss increased with increasing grinding time regardless of interlayer cation species. These results show that the prolongation of grinding time results in the increase in physical and dissociative adsorbed water [8], as well as the promotion of delamination and fineness described above. $K_{0.8}$-tae have no interlayer water molecules because of non-expandability so that all the weight loss of $K_{0.8}$-tae series are assigned to physical and dissociative adsorbed water. Dissociative absorbed water resulting from broken bonds on ground fracture surface is dehydrated at relatively higher temperatures while physical absorbed water can be dehydrated at lower temperatures [9]. Weight loss over 800 °C results from the removal of fluorides due to the thermal decomposition of mica crystals. In $Na_{0.8}$-tae series, interlayer water molecules are removed below 100 °C in one step to yield anhydrous mica phase [10]. The ground $Na_{0.8}$-tae samples also lost physical absorbed water at the same temperature range, so that the overall weight loss of this step increased with increasing grinding time. In addition, the weight loss at higher temperatures assignable to dissociative water increased with the prolongation of grinding time. In $Li_{0.8}$-tae series, interlayer water molecules are generally removed below 650 °C through three steps [10], however, the increase in absorbed physical and dissociative water molecules makes the stepwise dehydration process obscurer with the prolongation of grinding time.

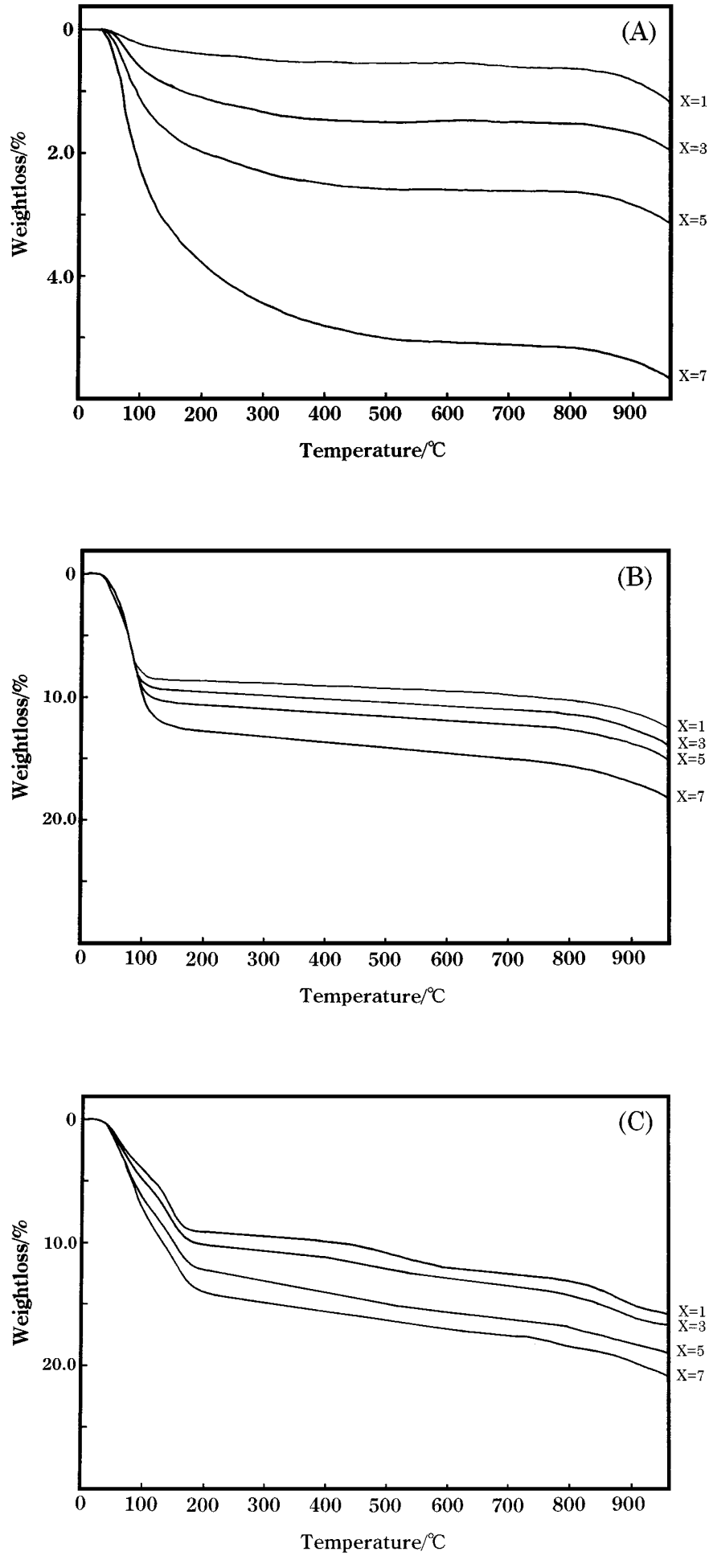

Figure 2 TG curves of $K_{0.8}$-, $Na_{0.8}$- and $Li_{0.8}$-taeniolite having different grinding times. (A) $K_{0.8}$-tae system, (B) $Na_{0.8}$-tae system, and (C) $Li_{0.8}$-tae system. The value of *x* shows the grinding time.

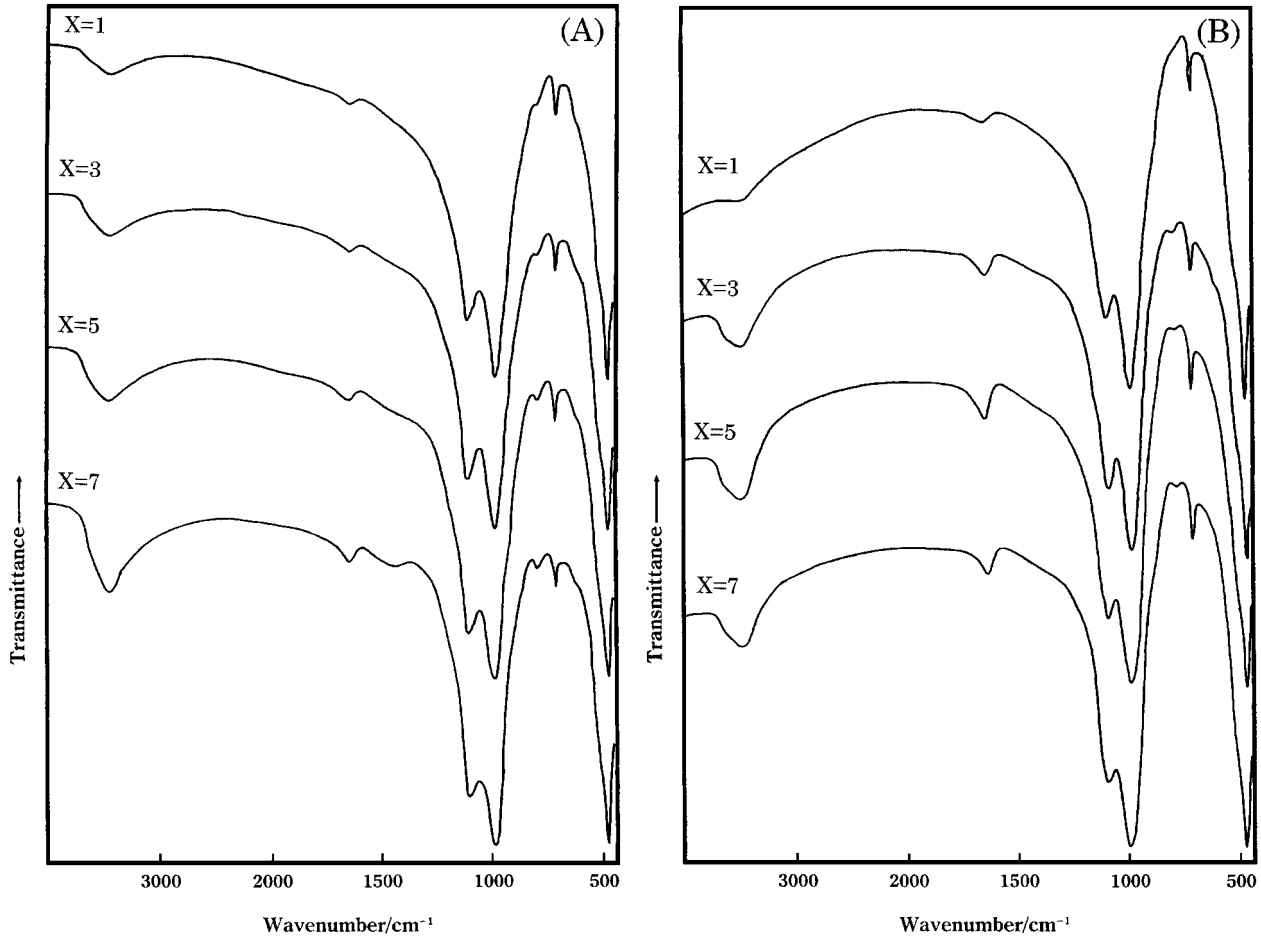

Figure 3 IR spectra of $K_{0.8}$- and $Na_{0.8}$-taeniolite having different grinding times. (A) $K_{0.8}$-tae system and (B) $Na_{0.8}$-tae system. The value of x shows the grinding time.

Fig. 3 shows infrared spectra of $K_{0.8}$- and $Na_{0.8}$-tae. The absorption bands at around 1000 and 1100 cm^{-1} are assignable to e_1^1 and a_1^1 mode, respectively, based on a $(Si_2O_5)_n$ normal vibration model [11–13]. The e_1^1 band involves Si-O_b (basal oxygen) vibrations while the a_1^1 band involves Si-O_a (apical oxygen) vibrations. These two bands showed no change with increasing grinding time, indicating that grinding caused no drastic change in the silicate structure of mica. However, as the grinding time was prolonged, the absorption bands at around 3450 and 1600 cm^{-1} became stronger. The former band is attributed to the stretching vibration while the latter to the deformation vibration of H_2O. These results indicate that absorbed water on mica crystals increases with increasing grinding time, corresponding to the results of TG analysis. Since the broadening [14] of absorption bands was undeveloped, the grinding under the present conditions didn't produce much amorphous phase [15, 16] from mica crystals. This is due to the moderate conditions of the grinding process employed. On the other hand, severe grinding under mechanical higher stresses made mica crystals transformed into amorphous phase. In montmorillonite or kaolinite, it is known that the proton transfer, i.e., so called prototropy, takes place from the interlayer water molecules or OH groups of the lattice to broken bonds of fresh fractured surfaces to form hydroxo groups. This prototropy effect may also contribute to increasing dissociative water in the present series of micas containing interlayer water molecules.

3.2. Properties of titania pillared fluorine micas obtained from ground host micas

Fig. 4 shows XRD patterns around the (001) diffraction region for titania pillared fluorine micas obtained from ground $Na_{0.8}$- and $Li_{0.8}$-tae. The (001) peak intensity of the titania pillared micas decreased with increasing grinding time. The peak position of (001) diffraction shifted to higher diffraction angles for $Na_{0.8}$-tae series and to lower angles for $Li_{0.8}$-tae series, respectively, with increasing grinding time. Judging from small angle scattering appearing below the diffraction angle of 4°, the regularity of stacking sequence for the layered structure of titania fluorine micas obtained from $Li_{0.8}$-tae series was lower than that obtained from $Na_{0.8}$-tae series. Titania pillared micas synthesized from $Na_{0.8}$- and $Li_{0.8}$-tae with longer grinding times lost the rationality of basal reflections (i.e., the regularity of stacking sequences represented by the equation; $d_{001} = 2 \times d_{002} = 3 \times d_{003} = \cdots$) and the high order reflections in XRD patterns. This suggests that the difference between the reactivities of the host micas and titania sol, which depend on the interlayer cation species at the initial stage of grinding, gradually diminishes

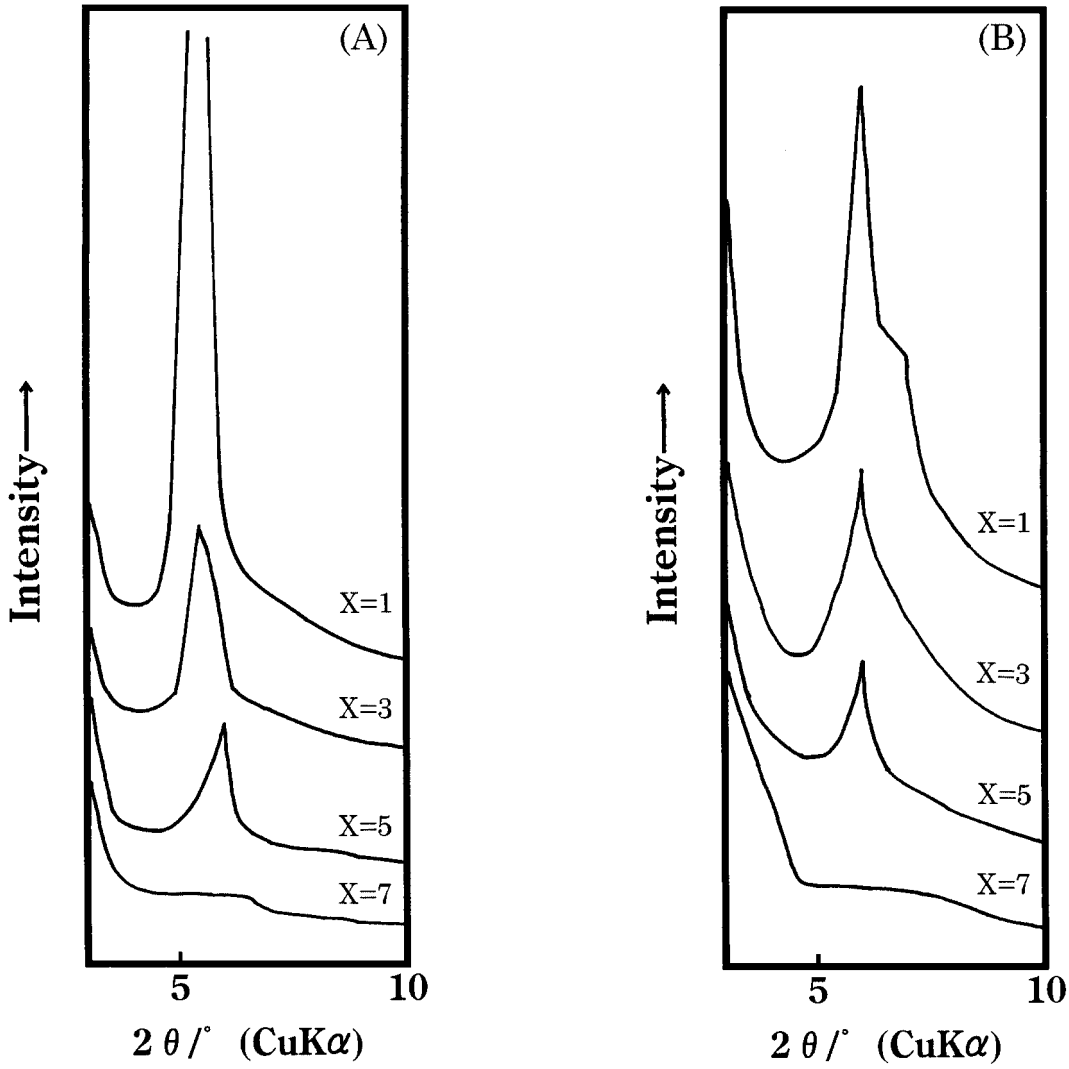

Figure 4 XRD patterns of various titania pillared fluorine micas obtained by drying in air. (A) $Na_{0.8}$-Ti-tae system and (B) $Li_{0.8}$-Ti-tae system. The value of *x* shows the grinding time of host crystals.

with the prolongation of grinding time and the observed basal spacing is an apparent value from the irregular stacking sequences. The irregularity of stacking sequences induced by grinding to the host crystals leads to the formation of more irregularly interstratified structures of the titania pillared micas through the course of the intercalation process.

Fig. 5 shows the specific surface areas (BET) of $Na_{0.8}$-Ti- and $Li_{0.8}$-Ti-tae series plotted against those of the ground host mica crystals. All the samples were heated at 150 °C prior to the measurements. Specific surface area of the titania pillared micas increased linearly with increasing surface area of the host crystals. The maximum specific surface area of $Na_{0.8}$-Ti-tae series was almost equal to that of $Li_{0.8}$-Ti-tae series, and the gradient of the specific surface areas for $Na_{0.8}$-Ti-tae series was larger than that for $Li_{0.8}$-Ti-tae series.

Fig. 6 shows the relation between titania contents and the specific surface area of the ground host mica crystals for $Na_{0.8}$-Ti- and $Li_{0.8}$-Ti-tae series. The samples are the same as shown in Fig. 5. Titania contents of the products increased with increasing surface area of the host crystals. The maximum titania content of $Na_{0.8}$-Ti-tae series was almost equal to that of $Li_{0.8}$-Ti-tae series. This corresponds to the change in the specific surface areas shown in Fig. 5. These results indicate that the formation and properties of titania pillared fluorine micas depend on not only interlayer cation species but also specific surface areas of host mica crystals, and the difference in properties between $Na_{0.8}$-Ti-tae and $Li_{0.8}$-Ti-tae almost diminishes with increasing specific surface area of host mica crystals. Based on the above discussion, it is concluded that titania is deposited on the external surfaces as well as in the interlayer regions of host mica crystals. Broken bonds [17] produced on cleavage planes and edges by grinding should contribute to the reaction for depositing titania on external surfaces.

When host crystals are larger, the contribution of intercalation predominates so that the formation and properties of titania pillared micas depend on expandability of host crystals, i.e., interlayer cation species [1]. On the other hand, the deposition on external surfaces becomes dominant when host crystals are finer. Consequently, the effect of interlayer cation species is diminished with increasing grinding time of host mica crystals while that of specific surface area becomes more and more important. Thus titania pillared micas obtained from well ground host mica crystals form so-called delaminated titania-pillared clays, [18, 19] or titania coated titania-pillared clays.

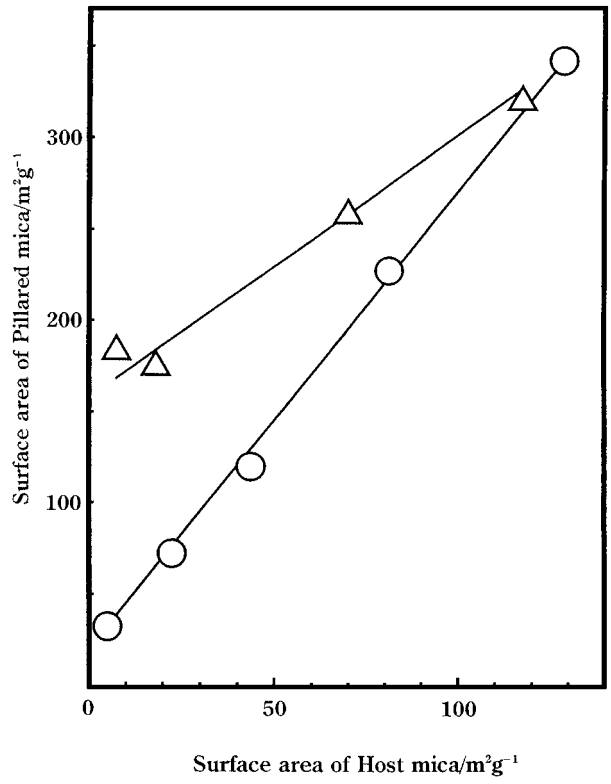

Figure 5 Relationship between surface area of host micas and that of titania pillared fluorine micas heated at 150 °C. ○: $Na_{0.8}$-Ti-tae system, △: $Li_{0.8}$-Ti-tae system.

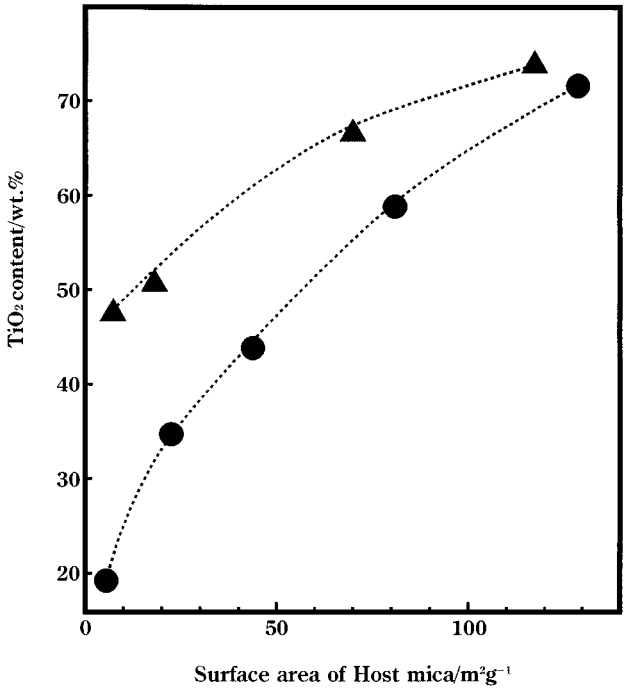

Figure 6 Relationship between surface area of host micas and titania content of pillared fluorine micas. ●: $Na_{0.8}$-Ti-tae system, ▲: $Li_{0.8}$-Ti-tae system.

The plausible reaction process on external surfaces is supposed as follows. Condensation reaction takes place between OH groups of external surfaces of host crystals and those of titania sols, giving hydroxotitanium compounds. Then the condensation-polymerization reaction proceeds between OH groups of hydroxotitanium compounds deposited on surfaces and those of titania sols. This successive process should increase titanium compounds deposited on external surfaces of titania pillared micas.

Fig. 7 shows the changes in basal spacings with increasing heat-treatment temperature for $Na_{0.8}$-Ti-tae and 5h-$Na_{0.8}$-Ti-tae. The observed basal spacing is an apparent average image of irregular stacking sequences. $Na_{0.8}$-Ti-tae gave the basal spacing of 1.50 and 1.26 nm at room temperature and in the temperature range from 200 to 300 °C, respectively, and collapsed to the 0.98 nm phase at 400 °C. On the other hand, 5h-$Na_{0.8}$-Ti-tae gave the basal spacing of 1.54 and 1.26 nm in the temperature range from room temperature to 200 °C

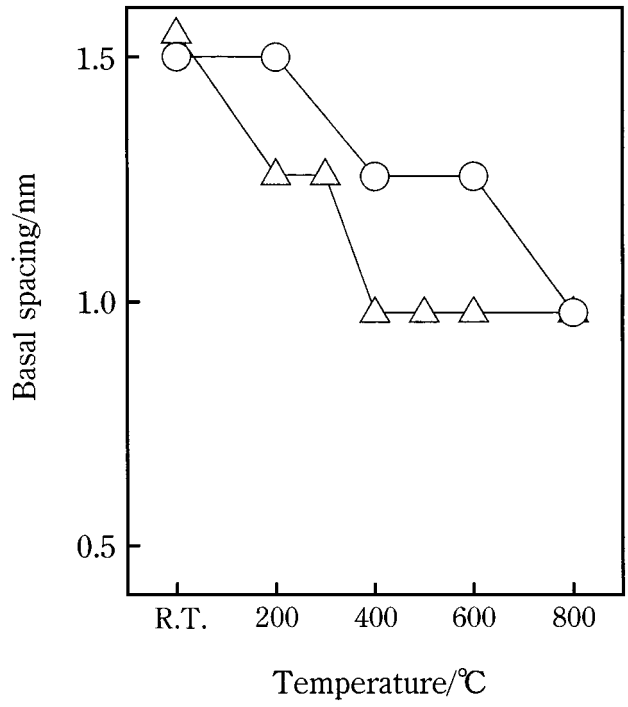

Figure 7 Basal spacings plotted against heating temperature for titania pillared fluorine micas. ○: 5h-$Na_{0.8}$-Ti-tae, △: $Na_{0.8}$-Ti-tae.

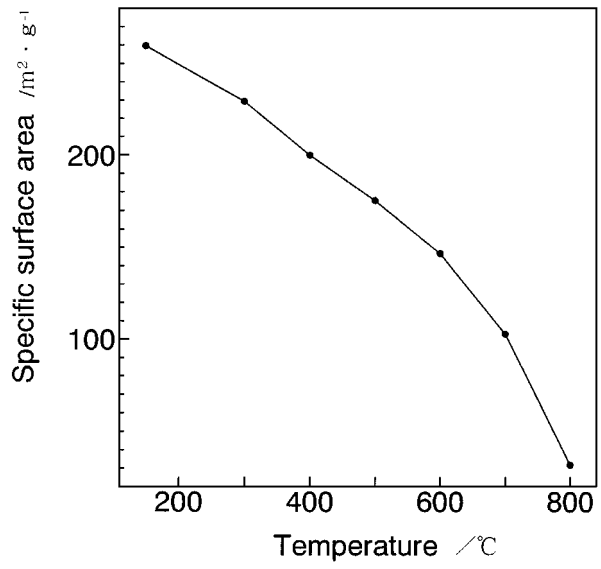

Figure 8 Specific surface area plotted against heat-treatment temperature for titania pillared mica (5h-$Na_{0.8}$-Ti-tae).

and from 400 to 600 °C, respectively, and collapsed to the 0.98 nm phase at 800 °C. The thermal durablity of 5h-$Na_{0.8}$-Ti-tae is higher than that of $Na_{0.8}$-Ti-tae. These differences in thermal behavior of titania pillared micas result from the difference in titania contents. The change in basal spacings with heat-treatment temperature for 5h-$Na_{0.8}$-Ti-tae is similar to that for $Li_{0.8}$-Ti-tae [1], supporting the fact that grinding of host crystals diminishes the effects of interlayer cation species upon the formation and properties of pillared micas.

Fig. 8 shows the relation between heat-treatment temperature and specific surface area for the titania pillared mica 5h-$Na_{0.8}$-Ti-tae. Specific surface areas decreased almost linearly up to 600 °C. 5h-$Na_{0.8}$-Ti-tae maintained its high surface area of 150 $m^2\ g^{-1}$ even at 600 °C, thereafter followed by the rapid decrease above 700 °C. This change in surface area above 600 °C corresponds to the collapse of basal spacings shown in Fig. 7.

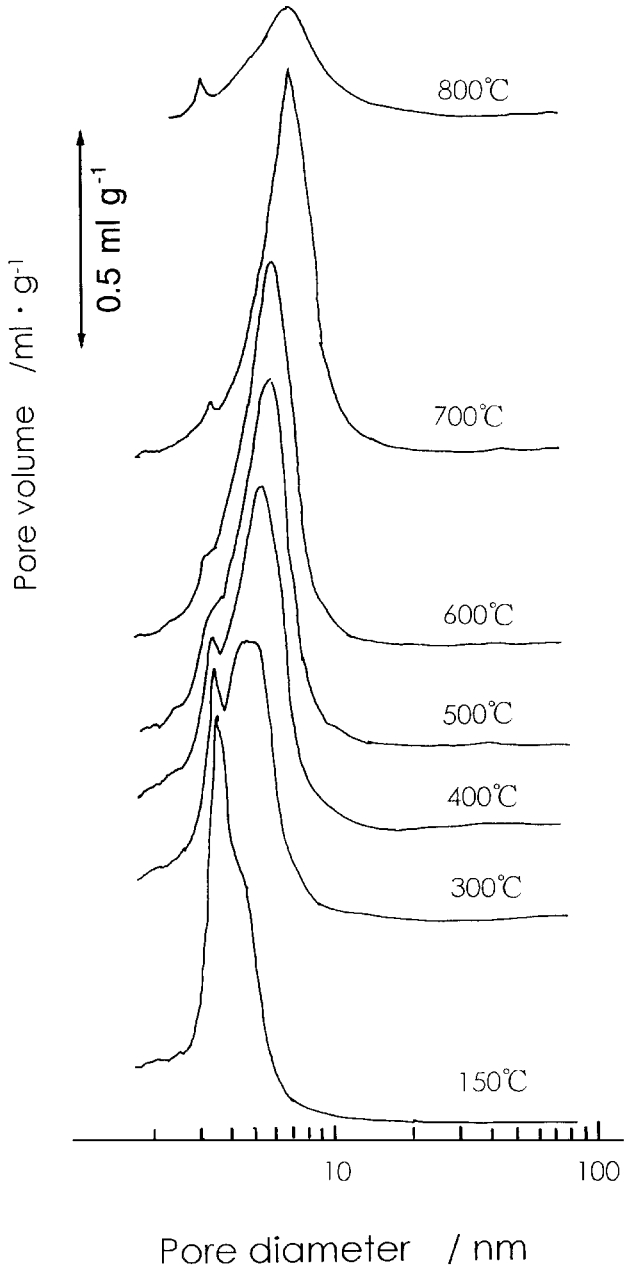

Figure 9 Pore size distribution curves for titania pillared mica (5h-$Na_{0.8}$-Ti-tae) obtained by heating at different temperatures.

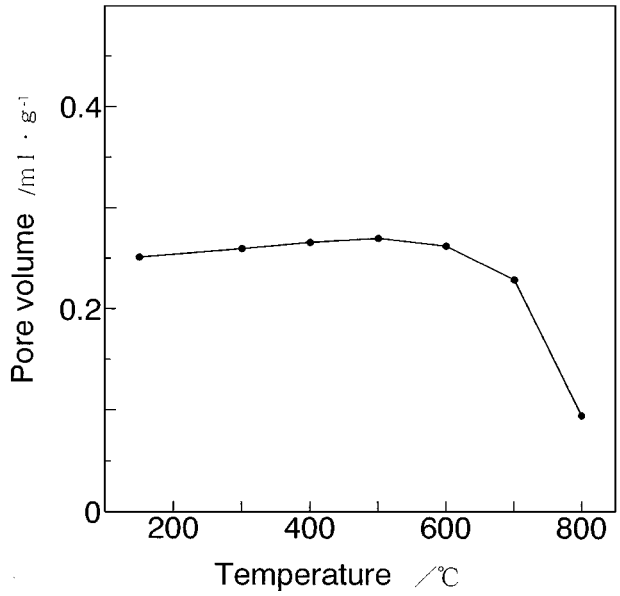

Figure 10 Total pore volume plotted against heat-treatment temperature for titania pillared mica (5h-$Na_{0.8}$-Ti-tae).

Fig. 9 shows pore size distribution curves for the titania pillared mica 5h-$Na_{0.8}$-Ti-tae heated at various temperatures. Total pore volume is plotted against heat-treatment temperature for the same pillared mica in Fig. 10. The sample heated at 150 °C gave a peak having a pore diameter of 3.2 nm. This peak is assignable to so-called slit pores which originate from the interstratified structure of pillared micas, and becomes weaker with increasing heat-treatment temperature. On the other hand, the shoulder having the pore diameter of about 4.5 nm at 150 °C shifted gradually to larger diameter sides to be a separated peak with increasing heat-treatment temperature, giving the pore diameter of 6.0 nm at 600 °C. This peak originates from the 'house of cards' structure [20] of delaminated pillared micas or titania coated titania-pillared mica flakes described above. The voids formed in the house of cards structure extended gradually due to the shrinkage of the coated titania layers with increasing heat-treatment temperature. However, the microstructure of pillared micas collapsed due to the initiation of thermal decomposition and sintering of titania over 800 °C, resulting in the rapid decrease in specific surface area. The total pore volume gave almost the constant value of 0.26 ml g^{-1} up to 600 °C, and decreased rapidly above 700 °C.

The pH value of titania sols before and after reaction with $Na_{0.8}$-tae and $Li_{0.8}$-tae are shown in Table I together with the reference system without adding mica

TABLE I pH of titania sols before and after reaction

	$Na_{0.8}$-Ti-tae-sol[a]	$Li_{0.8}$-Ti-tae-sol[b]	Ref-Ti-sol[c]
Before reaction	0.39	0.39	0.40
After reaction	0.30	0.30	0.29

[a]The sol used for obtaining titania pillared mica from unground $Na_{0.8}$-tae.
[b]The sol used for obtaining titania pillared mica from unground $Li_{0.8}$-tae.
[c]The sol used for reference experiment without mica.

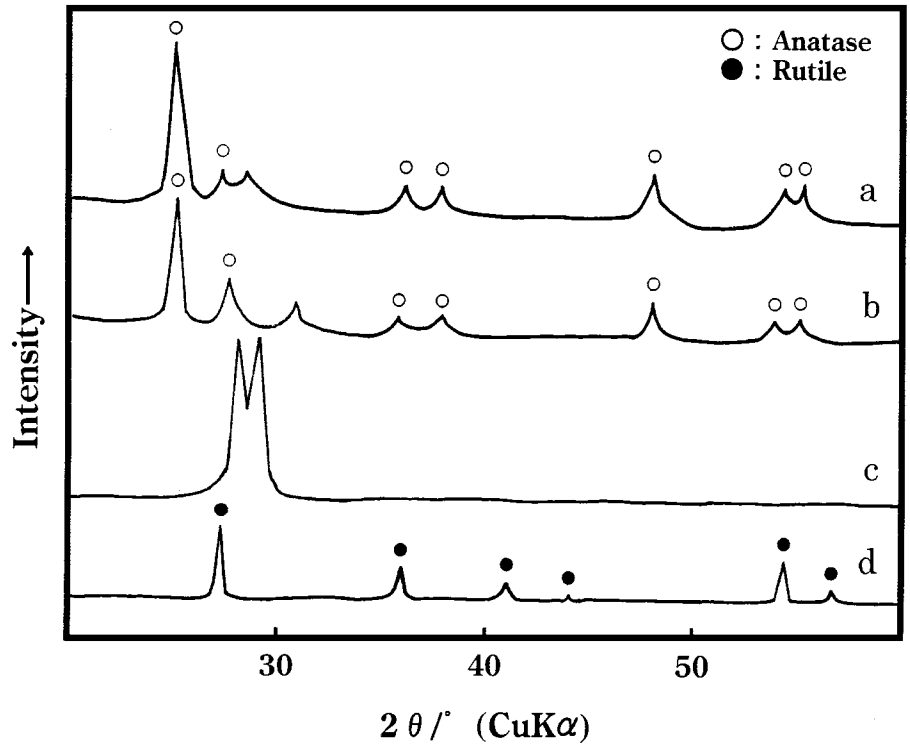

Figure 11 XRD patterns of titania pillared fluorine micas and titania obtained from the reference system by heating at 800 °C. (a) $Li_{0.8}$-Ti-tae, (b) 5h-$Na_{0.8}$-Ti-tae, (c) $Na_{0.8}$-Ti-tae and (d) obtained from Ti-sol (reference).

crystals. Fig. 11 shows XRD patterns of titania pillared micas and titania, which was obtained from the reference system, by heating at 800 °C. The changes in pH values of titania sols are almost the same among the three systems shown in Table I. The XRD patterns of 5h-$Na_{0.8}$-Ti-tae and $Li_{0.8}$-Ti-tae gave diffraction peaks assignable to anatase, although that of the reference system gave diffraction peaks ascribable to rutile. This indicates that the polytype of precipitated titania is determined by the coexistent mica phase since pH values are almost unchanged between the case using mica and that without mica. XRD pattens of $Na_{0.8}$-Ti-tae gave no peaks attributable to titania, indicating that the crystallization of titania phases depends on the titania content. Part of precipitated anatase originates from interlayer titania, which is expelled from the interlayer regions of pillared micas upon heating [1].

Machinable titania-mica sintered composite bodies could be prepared from titania pillared fluorine micas by molding at a pressure of 300 MPa followed by

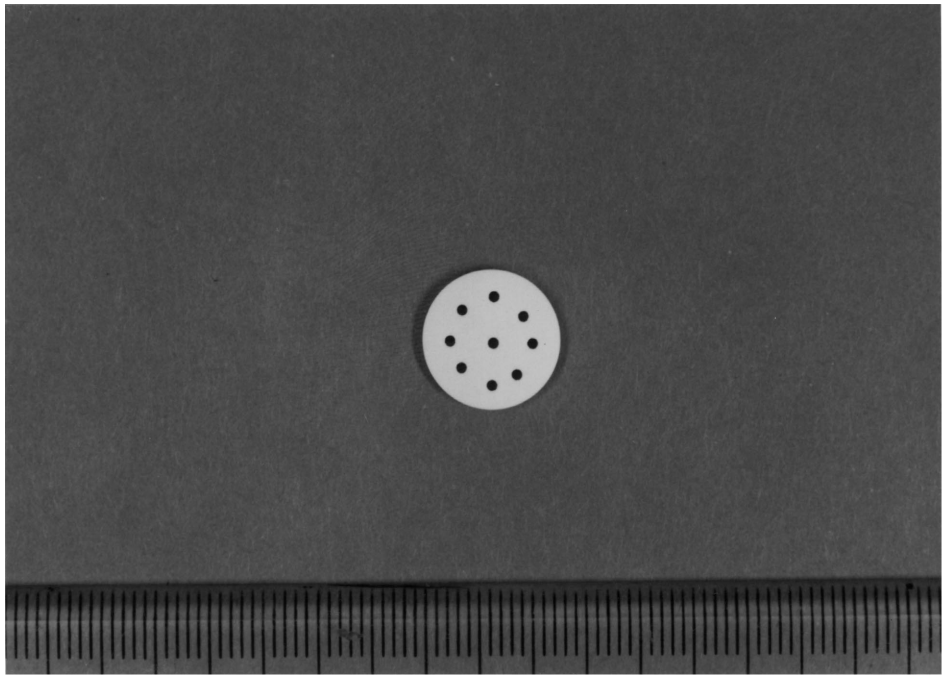

Figure 12 Sintered body of titania pillared mica showing machinability.

firing at 600–700 °C. The example of drilled specimens is shown in Fig. 12. Machinability should result from cleavability of mica flakes and the microstructure featuring the 'house of cards' structure.

4. Conclusion

Taeniolite series fluorine micas [$M_{0.8}Mg_{2.2}Li_{0.8}(Si_4O_{10})F_2$ (M = Na, Li)] having different grinding times were allowed to react with titania sol prepared by hydrolyzing titanium tetraisopropoxide (TTIP) with hydrochloric acid in order to clarify the reactivity of ground fluorine micas with titania sol. The results are summarized as follows:

1. When taeniolite series mica crystals were ground, the thermal weight loss and the relative intensity of IR absorption bands at 1600 and 3450 cm^{-1} became larger. The reason is that the prolongation of grinding time promotes delamination and fineness of mica crystals that is accompanied by the increase in physical and dissociative adsorbed water.

2. The properties of titania pillared fluorine micas obtained from ground host mica crystals depended on its grinding time. Specific surface areas and titania contents of titania pillared fluorine micas increased with increasing grinding time.

3. The difference in properties between $Na_{0.8}$-Ti-tae and $Li_{0.8}$-Ti-tae was almost diminished with increasing grinding time of host mica crystals. This is because titania deposits on external surfaces along with intercalation into the interlayer region of ground host mica crystals. These facts show that the prolongation of grinding time for host mica crystals leads not only to increasing surface areas but also changes in surface conditions and remarkably affects the formation and properties of the pillared micas.

4. The titania pillared micas obtained from well ground host micas with high surface areas formed so called delaminated pillared clays that exhibited mesoporous character and good machinability. The mesopores varied between 3.2–6.0 nm in diameter, depending on the heat-treatment temperature.

References

1. F. KUNIYOSHI and K. KITAJIMA, *Solid State Ionics* **101–103** (1997) 1099.
2. B. C. MACKENZIE and A. A. MILEN, *Mineral Mag.* **30** (1953) 178.
3. H. S. YODAR and H. P. EUGSTER, *Geochim. Cosmochim. Acta.* **8** (1955) 257.
4. B. CICEL and G. KRANZ, *Clay Miner.* **16** (1981) 151.
5. K. KITAJIMA, F. KOYAMA and N. TAKUSAGAWA, *Bull. Chem. Soc. Jpn*. **58** (1985) 1325.
6. S. YAMANAKA, T. NISHIHARA and M. HATTORI, *Mater. Chem. Phys.* **17** (1987) 87.
7. Japanese Industrial Standard, JIS M8311, 1967.
8. R. H. MUNCH, *J. Catal.* **3** (1964) 406.
9. K. SUZUKI, S. TOMURA and Y. KUWAHARA, *Funtai Kougaku Kaishi* **20** (1983) 122.
10. K. KITAJIMA, *Hyoumen* **19** (1981) 83.
11. M. ISHII, T. SHIMANOUCHI and M. NAKAHIRA, *Inorg. Chem. Acta.* **1** (1967) 387.
12. K. KITAJIMA, T. INADA and N. TAKUSAGAWA, *Seramikkusu Ronbunshi* **97** (1989) 649.
13. K. KITAJIMA and N. TAKUSAGAWA, *Clay Miner.* **25** (1990) 235.
14. T. TSUCHIDA and N. ICHIKAWA, *Reactivity of Solids* **7** (1989) 207.
15. J. CORNEJO and M. C. HERMOSIN, *Clay Miner.* **23** (1988) 391.
16. U. MINGELGRIN, L. KLIGER, M. GAL and S. SALTZMAN, *Clays Clay Miner.* **26** (1978) 299.
17. B. C. MACKENZIE and A. A. MILEN, *Clay Miner. Bull.* **2** (1953) 57.
18. J. P. CHEN, M. C. HAUSLADEN and R. T. YANG, *J. Catal.* **151** (1995) 135.
19. T. J. PINNAVAIA, M. TZOU, S. D. LANDAU and P. H. RAYTHATHA, *J. Mol. Catal.* **27** (1984) 195.
20. W. D. KINGERY, H. K. BOWEN and D. R. UHLMANN, in "Introduction to Ceramics" (John Wiley & Sons, New York, London, Sydney, Toronto, 1976) p. 555.

Received 20 April
and accepted 23 December 1998